Machine-Learning-based Monitoring and Optimization of Processing Parameters in 3D Printing

Article *in* International Journal of Computer Integrated Manufacturing · December 2022

DOI: 10.1080/0951192X.2022.2145019

Tariku Sinshaw Tamir
Guangdong University of Technology

Gang Xiong
Institute of Automation, Chinese Academy of Sciences

Qihang Fang
Institute of Automation, Chinese Academy of Sciences

Yong Yang
Chinese Academy of Sciences

International Journal of Computer Integrated Manufacturing

ISSN: (Print) (Online) Journal homepage: https://www.tandfonline.com/loi/tcim20

Machine-learning-based monitoring and optimization of processing parameters in 3D printing

Tariku Sinshaw Tamir, Gang Xiong, Qihang Fang, Yong Yang, Zhen Shen, MengChu Zhou & Jingchao Jiang

To cite this article: Tariku Sinshaw Tamir, Gang Xiong, Qihang Fang, Yong Yang, Zhen Shen, MengChu Zhou & Jingchao Jiang (2023) Machine-learning-based monitoring and optimization of processing parameters in 3D printing, International Journal of Computer Integrated Manufacturing, 36:9, 1362-1378, DOI: 10.1080/0951192X.2022.2145019

To link to this article: https://doi.org/10.1080/0951192X.2022.2145019

Published online: 17 Nov 2022.

INTERNATIONAL JOURNAL OF COMPUTER INTEGRATED MANUFACTURING
2023, VOL. 36, NO. 9, 1362–1378
https://doi.org/10.1080/0951192X.2022.2145019

Machine-learning-based monitoring and optimization of processing parameters in 3D printing

Tariku Sinshaw Tamir[a,b], Gang Xiong[a,c], Qihang Fang[a,b], Yong Yang[d], Zhen Shen[a,c], MengChu Zhou[e,f] and Jingchao Jiang[g]

[a]The State Key Laboratory for Management and Control of Complex Systems, Beijing Engineering Research Center of Intelligent Systems and Technology, Institute of Automation, Chinese Academy of Sciences, Beijing, China; [b]The School of Artificial Intelligence, University of Chinese Academy of Sciences, Beijing, China; [c]The Guangdong Engineering Research Center of 3D Printing and Intelligent Manufacturing, Cloud Computing Center, Chinese Academy of Sciences, Dongguan, China; [d]The State Key Laboratory of High Performance Ceramics and Superfine Microstructure, Shanghai Institute of Ceramics, Chinese Academy of Sciences, Shanghai, China; [e]Helen and John C. Hartmann Department of Electrical and Computer Engineering, New Jersey Institute of Technology, Newark, NJ, USA; [f]Macao Institute of Systems Engineering and Collaborative Laboratory for Intelligent Science and Systems, Macau University of Science and Technology, Macao 999078, China; [g]Department of Mechanical and Automation Engineering, The Chinese University of Hong Kong, Shatin, Hong Kong

ABSTRACT
Additive manufacturing (AM), commonly known as 3D printing, is a rapidly growing technology. Guaranteeing the quality and mechanical strength of printed parts is an active research area. Most of the existing methods adopt open-loop-like Machine Learning (ML) algorithms that can be used only for predicting properties of printed parts without any quality assuring mechanism. Some closed-loop approaches, on the other hand, consider a single adjustable processing parameter to monitor the properties of a printed part. This work proposes both open-loop and closed-loop ML models and integrates them to monitor the effects of processing parameters on the quality of printed parts. By using experimental 3D printing data, an open-loop classification model formulates the relationship between processing parameters and printed part properties. Then, a closed-loop control algorithm that combines open-loop ML models and a fuzzy inference system is constructed to generate optimized processing parameters for better printed part properties. The proposed system realizes the application of a closed-loop control system to AM.

ARTICLE HISTORY
Received 7 November 2021
Accepted 14 October 2022

KEYWORDS
Additive manufacturing; closed-loop; 3D printing; digital manufacturing; machine learning; processing parameters

1. Introduction

Generally, manufacturing is defined as an industrial production system through which raw material is changed into completed items to be sold in a market. The strategies for manufacturing can follow forming, casting, subtracting and additive processes (Esmaeilian, Behdad, and Wang 2016). Forming applies force to bring deformations on raw material such that the required shapes and sizes can be acquired while casting involves pouring liquid material into a mold (shaping device) and solidify it to make an object. Subtracting, on the other hand, makes an object by cutting or removing material away from a solid block of materials. Different from all of them, additive manufacturing (AM) makes an object by joining materials using a layer-upon-layer deposition approach.

AM (3D printing), as a supporting technology in social manufacturing and cloud manufacturing (Xiong et al. 2022), at its infancy was developed in the name of rapid prototyping. Initially, it is used to define architectural or anatomical production models (Camacho et al. 2018; Ngo et al. 2018). Next, the technology moves to rapid tooling allowing the fabrication of tools directly or indirectly such as injection molding, blow molding, and thermoforming applications and also for fabrication of electrical discharge machining electrodes (Uhlmann et al. 2018). Finally, the concept of AM moves to rapid manufacturing that can produce and realize fully functional products (Bikas, Stavropoulos, and Chryssolouris 2016).

In the era of AM, various types of AM technologies have been discovered and discussed, including fused deposition modeling, laser engineered net shaping, stereolithography, direct metal deposition, electron beam melting, selective laser melting, selective laser sintering, and wire and arc additive manufacturing (WAAM) (Zhao et al. 2018; Zhang et al. 2020). Those AM technologies require basic tasks including

CONTACT Zhen Shen zhen.shen@ia.ac.cn Institute of Automation, Chinese Academy of Sciences, No. 95 Zhongguancun E. Road, Beijing 100190, China

computer aided design (CAD) modeling, slicing, toolpath generation, part building, and post-processing. The quality of a 3D printed part is affected by each stage. Firstly, at the so-called slicing stage, the CAD model of an object is converted into a series of layers depending on the type of slicing strategies used. The most common and widely used slicing technique is planar slicing which slices the model into parallel layers. Subsequently, a toolpath is generated, which guides the motion of the print head in a printing process. Finally, the printed object is further enhanced by processes involving removal of support structures.

Optimizing and monitoring processing parameters is a tough and one key task in a 3D printing process since they determine the quality and mechanical strength of printed parts (Fang et al. 2023). Scientists and engineers are interested in constructing the direct linkage between process-structure and property-performance (P-S-P-P) (Popova et al. 2017; Wang et al. 2018a). However, due to the high nonlinearity of this linkage it is difficult to formulate an underlying mathematical expression for it. Therefore, taking the advantage of its intrinsic nonlinear behaviors, machine learning (ML) (Ghahramani et al. 2020; Ieracitano et al. 2020; Meng et al. 2020; Goh, Sing, and Yeong 2020) becomes an ideal solution to formulate these mathematical relationships in an entire AM process.

Most of the existing approaches dedicated to guarantee the quality and mechanical strength of printed parts generally depend on the prediction results that are normally obtained via open-loop-like ML algorithms. In such cases, only part properties are predicted without any correction mechanism in the presence of any printed part abnormalities. As a result, a part building process is not always going as planned and there may be inaccuracies such as geometric deviation, surface roughness, porosity, and poor interconnection between layers. Very few closed-loop-based ML models (Wang et al. 2018b), on the other hand, consider no more than one adjustable processing parameter to maintain the desired printed part properties. Therefore, a more reliable control design strategy that considers many adjustable processing parameters needs to be proposed. To create a complete full-scale AM system, it is necessary to design feedback control algorithms such that the system can compensate for the corresponding inaccuracies in a part building process. Maintaining the shape and size of a designed 3D object needs an intelligent feedback control loop; while online system parameter measurements are needed to ensure the current state of a printing process. Consequently, the control system can adjust processing parameters. In this study, both open-loop and closed-loop ML models are developed. The former is used to generate the relationship between processing parameters and printed part properties, which is useful to construct a closed-loop fuzzy inference system. Then a fuzzy-based feedback control system is used to optimize processing parameters.

Fuzzy logic was first coined by Lotfi A. Zadeh in 1965 (Zadeh 1965). Since then it has been used to model uncertain, linguistic and imprecise data (Liu et al. 2020; Wang et al. 2021). With its great interpretation capability, a fuzzy inference engine is being used as typical control techniques for non-linear systems (Di et al. 2001). Unlike the conventional ones (Tamir et al. 2020b,c), whose performance depends on the modeling accuracy of a physical system, a fuzzy control system is used when an analytical model is difficult to obtain while expert experience is available. Thus, it is wise to extend the controlling capability of a fuzzy system in manufacturing industry where experts' knowledge about a process is present while an analytical model is missing. Heidarzadeh et al. (2020) use fuzzy logic control to optimize the friction stir welding of pure copper. Li et al. (2021) prove the effectiveness of a fuzzy inference system for adjusting deposition parameters of beads in WAAM.

The remainder of the paper elucidates the state of the art for the applications of ML in AM industry, and design and implementation of control methods. Section 2 presents the researchers' perspectives on methods and approaches that are used to monitor the quality and mechanical strength of printed parts. As the core of this research work, Section 3 introduces the methods for machine learning and collection of datasets in the domain of AM. Section 4 presents feedback control algorithm implementation along with the mathematical expression of a 3D printer. Section 5 gives the results and discussions, followed by conclusions and perspectives in Section 6.

2. Related work

To assure the surface quality and mechanical strength of printed parts, various methods are reported in the literature. In the following paragraphs, we give their detailed review and elaborate how ML methods are involved to make improvement. The methods mainly focus on three ways to ensure the quality and mechanical strength of printed parts.

The first way is incorporating different pre-printing design techniques, such as an open-loop-based path design and support structure generation. Typical research in improving the mechanical strength of AM parts is reviewed as follows. Sugiyama et al. (2018) propose a method for manufacturing sandwich structures by a single piece composed of core shapes including honeycomb, rhombus, circle, and rectangle. The three-point bending test shows that increasing effective density yields maximum load and flexural modulus for all core shapes, but rhombus core shape is found to be the strongest. Bin Ishak, Fleming, and Larochelle (2019) suggest a robotic 3D printer to realize multi-plane layered path generation. The proposed printing approach improves the elastic modulus, ultimate tensile strength and yield the strength of the tensile specimen. Tamir et al. (2022a) propose a novel robot-assisted AM along with a control system framework, which possesses multi-directional printing without support structures. Huang and Singamneni (2015) propose an adaptive curved surface slicing algorithm combining flat and curved layers together. Their three-point bending test shows that the thicker curved layer leads to better mechanical strength. Lim et al. (2016) use planar and surface layer printing in a concrete 3D printing process; and conclude that surface layer printing yields higher strength. Xia, Lin, and Ma (2020) improve the mechanical performance of a printed object by constructing the toolpath in the direction of maximum principal stress.

Typical research in improving the surface quality of AM parts is summarized next. Jin et al. (2017) present a curved layer slicing algorithm to determine a printing path for a 3-axis 3D printer. In their approach, the stair-step effect that results in undesirable surface finish is reduced. Moreover, curved surfaces are accurately approximated by using B-spline. Isa and Lazoglu (2019) give a 5-axis path planning algorithm that minimizes staircase effects on solid and hollow printing part components. Their study subsequently checks path and tool orientation conditions. Ding et al. (2015) present a path planning algorithm that improves the quality and material efficiency in WAAM. Feng et al. (2018) propose a precise, reliable, and practically applicable slicing approach of T-spline surfaces. Similarly, Xie et al. (2020) propose a practically applicable, feasible, and effective spline-based smoothing algorithm to remove sharp corners around a printing path.

The second and third ways to guarantee quality and mechanical strength of printed parts are ML-based pre-process parameter optimization and ML-based in-situ monitoring, respectively. The former is an open-loop approach; while the latter is a closed-loop one. They are discussed next.

Li et al. (2019) propose a data-driven prediction model for the prediction of surface roughness in AM industry. To collect temperature and vibration data, various types of sensors, including accelerometers, thermocouples, and infrared temperature sensors, are used. Time and frequency domain data are extracted from the sensor to train an ensemble learning algorithm. Khanzadeh et al. (2018) present supervised machine learning algorithms to predict porosity within the printed parts from the morphological characteristics of melt pool boundary. A thermal monitoring system captures the melt pool signals, which may be labeled as either normal or pores by x-ray tomography. Francis and Bian (2019) develop a convolutional neural network-based geometric compensation mechanism that uses melt pool thermal history as input and distortion as output in a laser-based AM. Feeding back the distorted model to the original CAD model compensates geometric error. Similarly, a convolutional neural network-based 3D printing model error compensation framework is presented (Shen et al. 2019b; a; Zhao et al. 2019). It has two kinds of networks, i.e. a prediction network and a compensation network to yield a compensated model for a 3D printer. Wang et al. (2021) develop a regression model and layer time control method to improve product quality and efficiency of a large-scale AM. Their work uses real time print surface temperature data from an infrared camera. Tamir et al. (2022b) propose a feedback-based error compensation strategy, which integrates a fuzzy inference system and a grey wolf optimization algorithm. Wang et al. (2018b) propose a closed-loop control framework that integrates a vision-based technique and neural network (NN). It is able to inspect in-situ droplet behaviors and accordingly stabilize the printing process in liquid metal jet printing. Their study combines NN with a proportion-integration-differentiation (PID) control system to determine a drive voltage by taking droplet-image features and properties as the training dataset. A comprehensive review of AM process monitoring, diagnosis and control can be found in (Fang et al. 2023).

We intend to investigate two key issues from the aforementioned literature: 1) how to model an open-loop ML for prediction (Li et al. 2019; Khanzadeh et al. 2018), and 2) how to design an ML-based closed-loop control system (Wang et al. 2018b, 2021). We aim to propose a novel system that integrates open-loop ML models and a fuzzy inference system for processing parameter optimization, which is never seen before to our best knowledge. Matlab simulation is done for the purpose of verification.

3. Design of ML algorithms and dataset generation

3.1. Data collection

ML algorithms are data-driven approaches whose performance are highly dependent on the amount of data. In some areas, researchers tend to construct their own training datasets, such as SQuAD for natural language processing, ImageNet for image recognition, YouTube-8 M for video classification, and MNIST for optical character recognition (Qi et al. 2019). As a result, the potential of ML is highlighted in those areas. On the contrary, AM lacks organized experimental datasets due to high cost of collecting data. This discourages interested parties to build an open access dataset. Data collection remains an unsolved problem and becomes a challenge for those AM practitioners and researchers who are interested in applying ML.

To ensure an advanced AM technology, sensors are supposed to be placed in a printing process loop to capture data, such as geometric deviation, surface roughness, and porosity. A data collection sensory system can be implemented by either offline, online, or sometimes both. In an offline case, a necessary printed part geometrical information is measured after the completion of an entire printing process. Microscope is ideal equipment to highlight the desired information. While online sensory system actions are in-situ measurements through which data are collected during a printing process. A 3D camera can be used to capture a real time printing information in this case. Both offline and online sensory systems can be applied. The former is used to model an ML algorithm for quality prediction and the latter is used in an online processing parameter optimization.

This study uses the collected dataset from other work. The work (Jiang et al. 2020) uses the data to

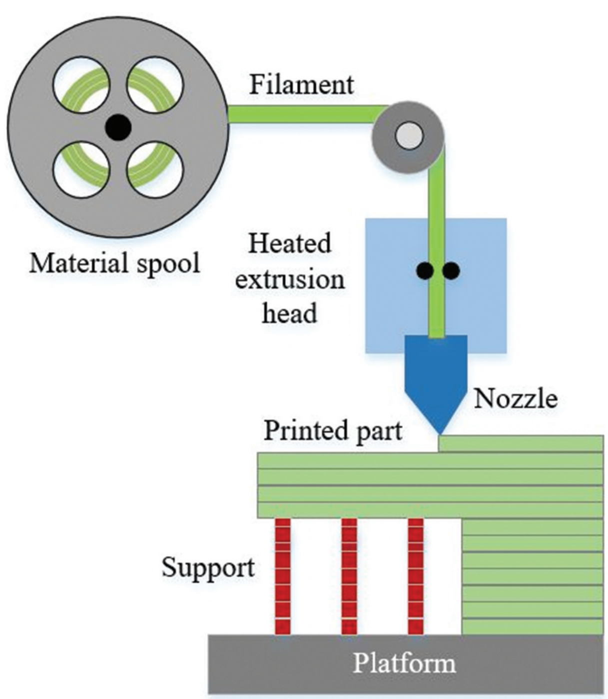

Figure 1. Fused deposition modeling system.

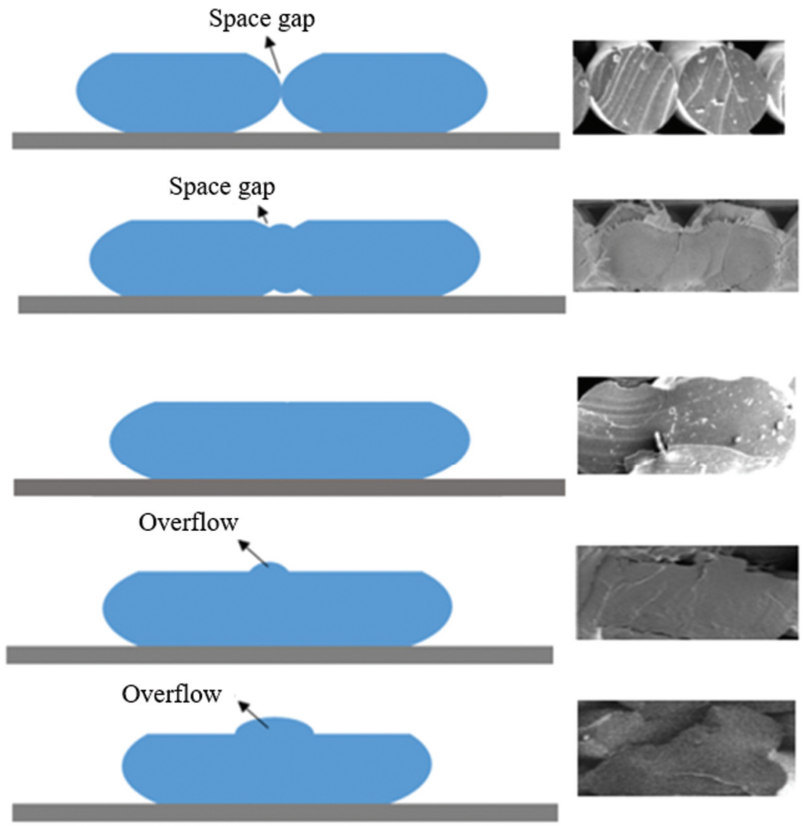

Figure 2. The experimental images showing connection status between printed lines (Jiang et al. 2020).

build up an ML model for AM prediction. Its data is uploaded to GitHub (Jiang 2019) for others to use. Different from (Jiang et al. 2020), we use the data to design an ML-based open-loop and closed-loop prediction system for monitoring and optimization of AM. As a part of a data collection method, they use an offline sensory system to record the processing parameters versus printed part properties. Fused deposition modeling type 3D printer is used to conduct a printing experiment as shown in Figure 1. The experimental real images are shown in Figure 2. Four adjustable processing parameters, i.e. layer height, print speed, line distance, and filament extrusion speed, are used. They are utilized to determine a connection status among printed lines. The connection status comprises of five classes – class 0 for large space, 1 for little space, 2 for good connection, 3 for little material overflow, and 4 for large material overflow – as shown in Figure 3. The class label is given based on space between two consecutive printed

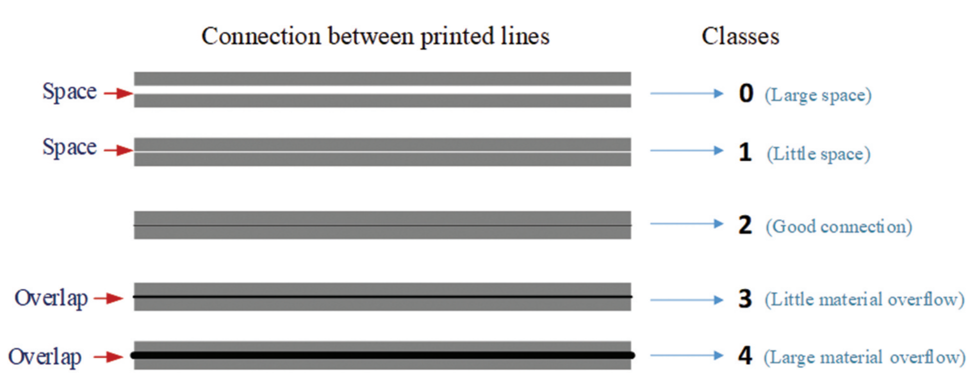

Figure 3. Class assignment for printed line connection.

Table 1. Experimental samples.

No.	Filament extrusion speed (mm/s)	Layer height (mm)	Line distance (mm)	Print speed (mm/s)	Classes
1	0.5	0.1	0.3	10	4
2	0.5	0.2	0.3	10	3
3	1	0.1	0.9	10	2
4	1	0.2	0.9	20	0
5	1.5	0.4	0.5	40	0
6	1.5	0.1	0.3	40	1
7	2	0.1	0.3	10	4
8	2	0.3	0.7	10	2
9	2.5	0.2	0.3	30	3
10	2.5	0.2	0.5	50	1

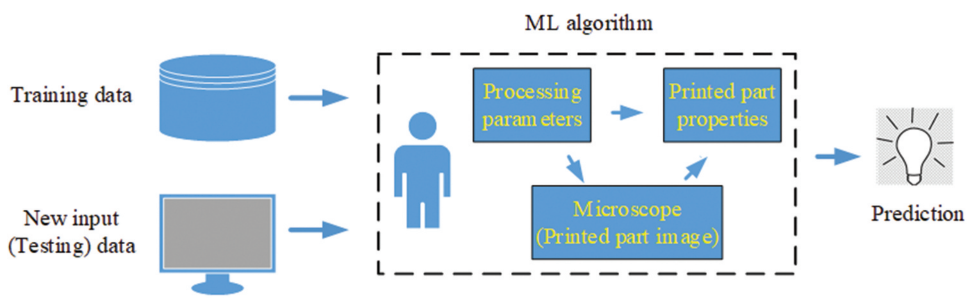

Figure 4. Open-loop-based (offline) optimal parameter settings.

lines. Either high spacing or overlapping between two lines tells us about a poor connection, whereas acceptable spacing is called a good connection. 400 labeled data are generated from the experiment, some of which are shown in Table 1. Note that mm and mm/s stand for millimeter and millimeter-per-second, respectively.

3.2. Open-loop control system

In control theory, open-loop and closed-loop control systems are the two popular algorithms implemented in a control engineering application area (Mei et al. 2021). The former uses no feedback to generate control actions. On the other hand, the latter uses feedback as a vital component for controlling a system. The proposed ML classification algorithms in this section take processing parameters as input and predict printed part properties without any correction mechanism to handle printed part abnormalities. Rather, they give knowledge to determine optimal parameters for better part quality. Generally, this process is categorized under an open-loop system since it cannot regenerate new parameters dynamically. This open-loop-like ML system is a human-in-the-loop system since training and testing data are generated by a human operator. The overall structure of the system is shown schematically in Figure 4.

3.3. Design of ML algorithms

ML is a rapidly growing technology applicable to analyze complex systems where mathematical representation is a challenge. It has also an ability to learn tasks with no explicit programming (Geron 2018; Moe, Rustad, and Hanssen 2018; Khargonekar and Dahleh 2018). The most known types of ML are supervised learning, unsupervised learning, transfer learning, and reinforcement learning (Cao, Lin and Zhou 2021; Wang et al. 2018a; Goodfellow et al. 2016; Tamir et al. 2020a; Yao et al. 2022). In a supervised learning, datasets are presented in a vector form of (x, y) and the aim is to predict output data y given input data x. An ML model is trained by using training data and then used to predict the values of new input data.

In this study, five supervised ML algorithms – deep neural network (DNN), support vector machine (SVM), decision tree (DT), random forest (RF), and logistic regression (LR) – are used for classification. The resulting models are used to decide the status of printed line connection given layer height, print speed, line distance and filament extrusion speed.

DNN is a special type of NN with many layers having basic processing elements called neurons. The connection of neurons in a layer forms a network. Each neuron performs its activation function given a weighted sum of its inputs and a bias. The following

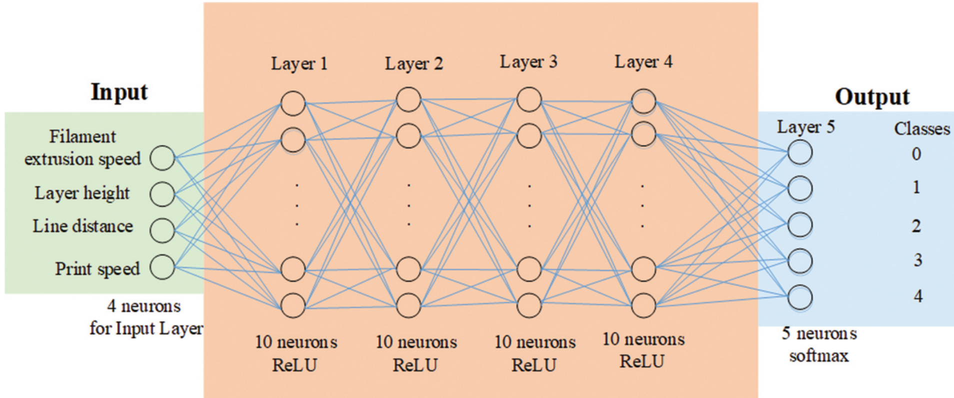

Figure 5. The structure of DNN3.

equation presents the result of an output neuron of an entire network:

$$y = f\left(\sum_{i=1}^{n} w_i x_i + b\right) \tag{1}$$

where y is the output of the neuron, x is its input, $w = (w_1, w_2, \ldots, w_n)^T$ is a weight vector and b is a bias. Weights and biases are the NN parameters which need to be updated during an NN training process. The combination of neurons in a typical NN forms three layers, including input, hidden, and output layers. If the number of hidden layers is more than one, a network is called DNN. This study uses three DNN architectures. One of them called DNN3 is shown in Figure 5, which is composed of four hidden layers. Figure 5 shows the overall network connection and the number of neurons in each layer with the corresponding activation function. For the first four layers, the rectified linear unit (*ReLU*) activation function is used, i.e.

$$ReLU(z) = max(z, 0) = \begin{cases} z, z > 0 \\ 0, otherwise \end{cases} \tag{2}$$

It returns an output equivalent to an input for positive input values; and otherwise zero for all other input values. The SoftMax activation function is used in the last layer. The SoftMax function is a kind of probabilistic approach that normalizes all the values into the range $(0, 1)$ and the sum is equal to one. As a result, it is suitable for multi-level classification problems. Its mathematical expression is:

$$\sigma(z)_j = \frac{e^{z_j}}{\sum_{k=1}^{K} e^{z_k}} \tag{3}$$

where z is a real number, and again, j indexes the output units, so $j = 1, 2, \ldots, K$.

The loss function used in our designed DNN is categorical cross-entropy, i.e.

$$H(y, \hat{y}) = -\frac{1}{n}\sum_{i=1}^{n}\sum_{j=1}^{5} y_{ij} \ln\left(\hat{y}_{ij}\right) \tag{4}$$

where, y, $\hat{y}$ and n are the predicted output, actual output, and number of input samples respectively. y_i is the predicted output vector of the i^{th} sample, e.g. $[0.1, 0.1, 0.1, 0.6, 0.1]$, and y_{ij} is the j^{th} element of y_i, e.g. $y_{i4} = 0.6$. The Adam optimizer is used in an entire training process, and also 'accuracy' is chosen as a metric in this model. The batch size and number of epochs is set as 32 and 500, respectively.

4. Closed-loop ML system design

The application of an ML-based closed-loop control system in AM industry is becoming one leading innovation that significantly improves a printed part's quality. A feedback control algorithm decides the relationship between processing parameters and printed part properties in a 3D printing process and tunes the optimal processing parameters. And the aim of the feedback control system is to bring the connection status of class 2 in a possible way. Figure 6 shows the schematic view of the proposed control system along with the processing flow path. It consists of camera, ML models, a Fuzzy Logic Controller (FLC), and an extruder system. The camera captures an actual connection among printed lines, which is then compared with the ML model's output given the corresponding processing parameters. The comparator

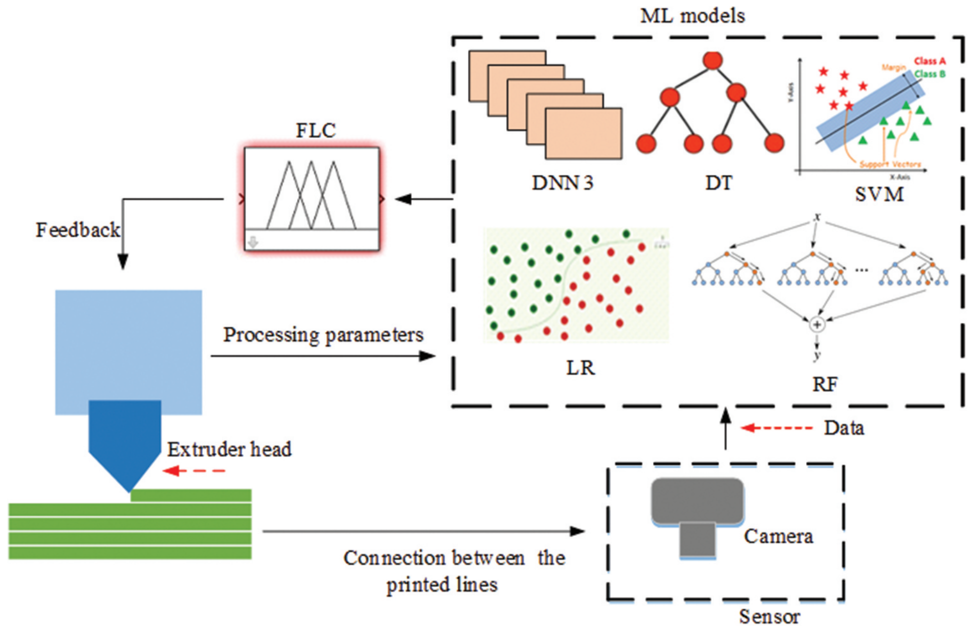

Figure 6. The proposed negative feedback control system in 3D printing.

outputs, i.e. the error and its derivative, are fed to FLC. Subsequently, FLC drives the extruder system with the optimized processing parameters. Priori-knowledge about the relationship between processing parameters and printed part properties formulated by an open-loop ML is used to construct a fuzzy inference system.

This work proposes a Multi-Input-Multi-Output (MIMO) Fuzzy logic-based control algorithm to generate optimized processing parameters. The fuzzy system takes 'error' and 'change in error' as inputs and outputs four processing parameters – filament extrusion speed, layer height, layer distance, and print speed as shown in Figure 7. In a fuzzification procedure, the triangular membership function is chosen to take the advantage of its simple calculation. The range of fuzzy membership functions is determined by a trial-and-error procedure. A Mamdani type fuzzy inference system (Prieto-Entenza et al. 2019) is applied. The

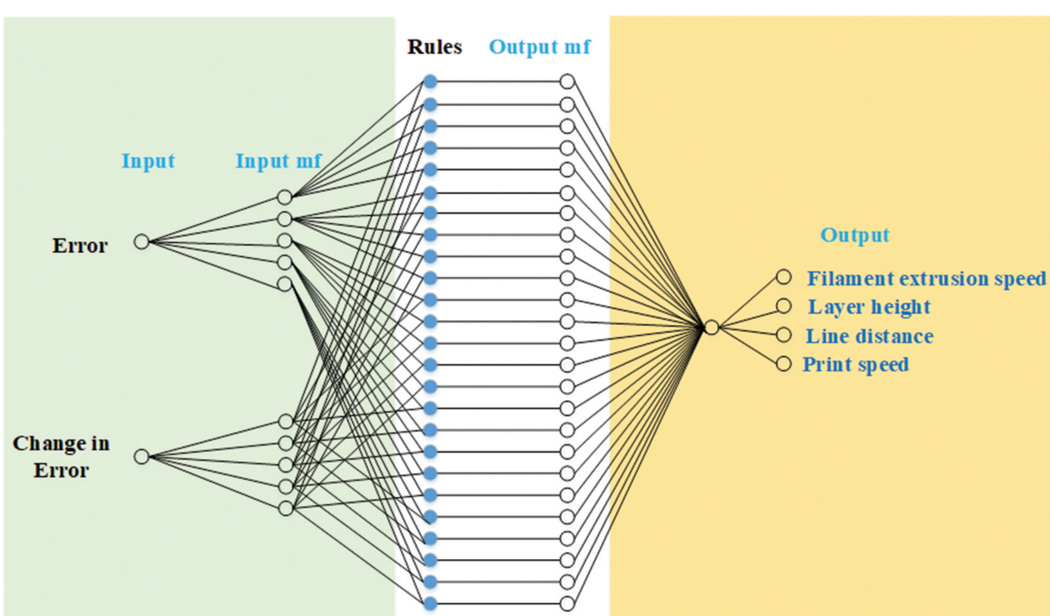

Figure 7. The fuzzy system structure.

inference system operations are fixed as 'And-Min', 'Implication-Min', 'Aggregation-Max, and 'Centroid' type of defuzzification. We design twenty-five IF … THEN structured fuzzy rules generated from two linguistic input variables. Each has five linguistic values. The five linguistic values are: negative-large, negative-small, zero, positive-small, and positive-large. Similarly, each of the four linguistic output variables have five linguistic values, including level-1, level-2, level-3, level-4, and level-5. The 'level' notation indicates that the range of the values. Figure 7 presents the overall structure of the designed fuzzy system that shows the interconnection of each linguistic values to form a set of fuzzy rules.

The designed fuzzy system is realized in algorithm 1 and implemented in Matlab Simulink environment. First, it reads the connection status and calculates 'Error' and 'Change in Error' accordingly. Subsequently, new optimized 3D printer processing parameters are computed recursively. The algorithm has two objective functions, 'Error' $E(x)$ and 'Change in Error' $\frac{dE(x)}{dt}$ as function of processing parameters. In fact, the error is expressed as the difference between reference connection status and actual connection status values. The setting of processing parameters directly affects the connection status values. Thus, even though there is no an equation that depicts the direct relationship between the error and processing parameters, the setting of processing parameters affects the error and it can be said that the relationship is involved indirectly. By applying the chain rule, the change in error can be expressed as:

$$\frac{\mathrm{d}E(x)}{\mathrm{d}t} = \frac{\partial E}{\partial x_1}\frac{\partial x_1}{\partial t} + \frac{\partial E}{\partial x_2}\frac{\partial x_2}{\partial t} + \frac{\partial E}{\partial x_3}\frac{\partial x_3}{\partial t} + \frac{\partial E}{\partial x_4}\frac{\partial x_4}{\partial t} \tag{5}$$

The aim of our optimization problem is to minimize two objective functions by finding optimized processing parameters. This can be written mathematically as:

$$\begin{aligned} &\min\ F(x) = \left[E(x), \tfrac{\mathrm{d}E(x)}{\mathrm{d}t}\right]^T \\ &s.t. \\ &\qquad x > 0 \end{aligned} \tag{6}$$

where $F(x)$ is a column vector of the two objective functions, and $x = (x_1, x_2, x_3, x_4)^T$ represents four processing parameters.

Algorithm 1: Optimization of processing parameters

Input: Error, $E(x)$, and Change in Error, $\frac{\mathrm{d}E(x)}{\mathrm{d}t}$, are FLC inputs, and Processing Parameters, *PP*, are MVLR inputs
Output: Processing Parameters, *PP*, are FLC outputs, and Connection Status, *CS*, is MVLR output
Initial Processing Parameters, *IPP*;
Reference Connection Status, RCS;
while *the 3D printer is running* **do**
  Read *CS*;
  Compute $E(x) = RCS - CS$;
  Compute $\frac{\mathrm{d}E(x)}{\mathrm{d}t}$;
  if $E(x)$ *and/or* $\frac{\mathrm{d}E(x)}{\mathrm{d}t}$ *are/is either large or medium* **then**
    New *PP* = updated *PP*;
  else
    New *PP* = *IPP*;
  end
  Return New *PP*;
end

In addition to closed-loop control system design, the mathematical expression of a 3D printer is necessary to ensure the state of a fully controllable condition. The system performance can be then verified in Matlab Simulink environment. Basically, two known modeling techniques, i.e. linear and nonlinear ones, are used to mathematically model the process. The former includes a transfer function, single-variable linear regression, and multi-variate linear regression. The latter includes state-space representation, single-variable higher order polynomial regression, and multi-variate higher order polynomial regression (Goodfellow et al. 2016). The former is applied for systems having inputs which are independent of each other, and the system output is then affected by individual inputs separately. The latter, on the other hand, is used when system inputs have some sort of correlation to each other, and the way how those inputs affect an output is then treated in a different manner. In our case, the variables that are input to the system are uncorrelated to each other and their summed-up effect determines the output variable condition. As one of the linear modeling techniques, a Multi-Variate Linear Regression (MVLR) model can be used to represent the mapping of processing parameters to 3D-printed part properties. The general mathematical expression of MVLR is:

$$Y = \begin{bmatrix} y_1 \\ y_2 \\ \cdot \\ \cdot \\ \cdot \\ y_n \end{bmatrix} = \begin{bmatrix} 1 & x_{11} & x_{12} & \cdot & \cdot & \cdot & x_{1k} \\ 1 & x_{21} & x_{22} & \cdot & \cdot & \cdot & x_{2k} \\ \cdot & \cdot & \cdot & \cdot & \cdot & \cdot & \cdot \\ \cdot & \cdot & \cdot & \cdot & \cdot & \cdot & \cdot \\ \cdot & \cdot & \cdot & \cdot & \cdot & \cdot & \cdot \\ 1 & x_{n1} & x_{n2} & \cdot & \cdot & \cdot & x_{nk} \end{bmatrix} \begin{bmatrix} \beta_1 \\ \beta_2 \\ \cdot \\ \cdot \\ \cdot \\ \beta_{k+1} \end{bmatrix} + \begin{bmatrix} \varepsilon_1 \\ \varepsilon_2 \\ \cdot \\ \cdot \\ \cdot \\ \varepsilon_n \end{bmatrix} \tag{7}$$

In a simplified form, equation (7) can be expressed as:

$$Y = X\beta + \varepsilon \tag{8}$$

where Y is an $n \times 1$ output feature matrix, X is an $n \times (k+1)$ input feature matrix, β is an $(k+1) \times 1$ input feature coefficient matrix, and ε is an $n \times 1$ regression error matrix. k is the number of input features and n is the number of training examples. This work uses four input features and one output feature to build an MVLR model. Filament extrusion speed, print speed, layer height, and line distance are categorized under input features, whereas the connection status between two printed lines is categorized under an output feature. The total number of training examples is 400.

The regression error can be compensated by adding a random $n \times 1$ compensation matrix $\tilde{\varepsilon}$ in the left-hand side of equation (8) , thus resulting in:

$$Y + \tilde{\varepsilon} = X\beta + \varepsilon \tag{9}$$

Input features' coefficient matrix β can be expressed as:

$$\beta = X^{\dagger}(Y + \tilde{\varepsilon} - \varepsilon) \tag{10}$$

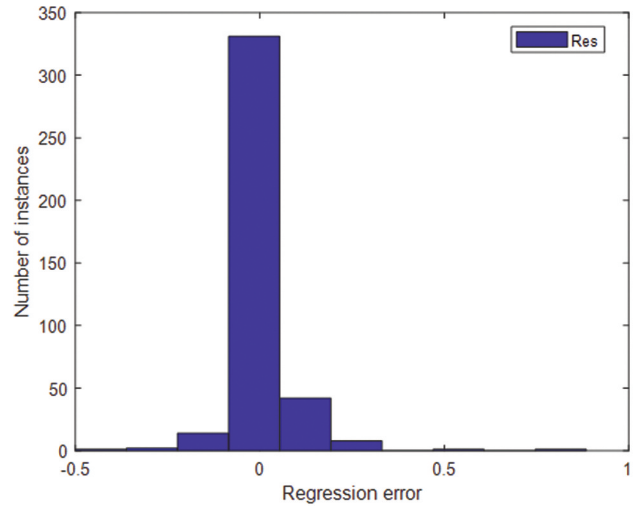

Figure 8. Regression error histogram.

where $X^{\dagger}$ is the pseudo-inverse of X. To minimize the effect of regression error on the MVLR model, we approximate $\tilde{\varepsilon}$ as ε, and compute β via equation (10). β is then in the form of $\beta = (\beta_1, \beta_2, \beta_3, \beta_4, \beta_5)^T$. Therefore, the final MVLR model describing a 3D printer is derived from equation (7) and mathematically expressed as:

$$Y = \begin{bmatrix} y_1 \\ y_2 \\ \cdot \\ \cdot \\ \cdot \\ y_n \end{bmatrix} = \begin{bmatrix} 1 & x_{11} & x_{12} & x_{13} & x_{14} & \\ 1 & x_{21} & x_{22} & & x_{23} & x_{24} \\ \cdot & \cdot & \cdot & \cdot & \cdot & \\ \cdot & \cdot & \cdot & \cdot & \cdot & \\ \cdot & \cdot & \cdot & \cdot & \cdot & \\ 1 & x_{n1} & x_{n2} & x_{n3} & x_{n4} & \end{bmatrix} \begin{bmatrix} 4.3520 \\ 0.4975 \\ -0.0564 \\ -3.3700 \\ -2.5450 \end{bmatrix} \tag{11}$$

The regression error histogram of the formulated MVLR model is shown in Figure 8. The distribution of

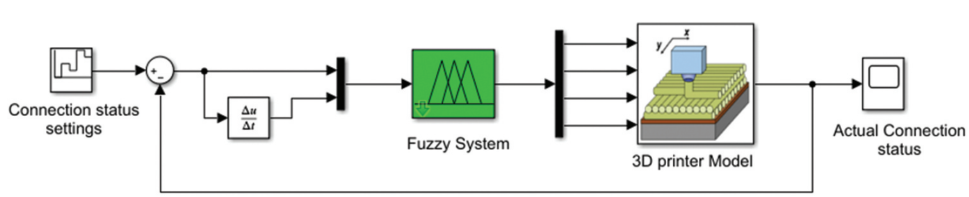

Figure 9. Simulink Model of 3D printing control system.

residues (Res) for the number of instances is observed in it. For most of the instances the error falls into the interval between −0.1 and 0.05. The mean squared error is found to be 0.0064 and this can be assumed as a tolerated error value. Therefore, we can use this type of model to approximate a real system. The Simulink model of a feedback fuzzy system along with the mathematical expression of a 3D printer is shown in Figure 9.

5. Results and discussions

5.1. Open-loop classification analysis

In this section, the open-loop classification results and discussions are presented. We choose five commonly used ML models, including DNN, SVM, DT, RF, and LR and present their performance. For each model, we first separate the data to two parts. 80% of the data are used for 5-fold cross-validation and 20% are used for model testing. Data in 5-fold cross-validation are further separated to five parts. Each part serves as the validation data once and the model is trained on the rest parts. From 400 samples, there are 205, 74, 52, 39, and 30 samples from label 1 to label 5 respectively. When the whole dataset is split randomly to training and testing data, for example, it is highly probable that the training data includes very few samples of label 5 (e.g. 2 samples), and the rest 28 samples of label 5 are included in the testing data. In this case, the trained model can work poorly. Therefore, each category of labels needs to be split independently as shown in Table 2. In cross-validation, we train each model five times and the validation accuracy for each model is recorded at each time. After cross-validation, for each model, we obtain a list of validation accuracy (V), i.e. V_1, V_2, V_3, V_4, and V_5.

Three DNN architectures are used – DNN1-DNN3. The architecture difference comes from the number of hidden layers used, as illustrated as follows. DNN1 has structure of (4, 10, 10, 5), which means the NN has 4 neurons in the input layer, 10 neurons in the first layer, 10 neurons in the second layer, and 5 neurons in the output layer. Similarly, DNN2 and DNN3 have structure of (4, 10, 10, 10, 5) and (4, 10, 10, 10, 10, 5) respectively. Table 3 shows validation accuracy of the individual folds and mean validation accuracy of each model.

The 5-fold cross-validation classification accuracy results for each model shown in Table 3 are used to choose the best model for final classification. Based on mean validation accuracy recorded in each model, it is observed that DNN with architecture DNN3 outperforms all other models with mean validation accuracy of 98.42%. On the contrary, LR scores the least mean validation accuracy of 89.96%. Moreover, from the DNN architectures, DNN1 scores the least mean validation accuracy of 98.13%. Therefore, DNN3 is chosen as the viable classification model for our task. Then a new DNN3 model is created and trained by using the whole dataset that was used for 5-fold cross-validation. As a result, the training accuracy of the new DNN3 model is achieved at 98.74%. Finally, the re-trained DNN3 model is used as the final model to do the testing with 20% of the whole data, and has reached testing accuracy of 97.53%. Compared to the training accuracy of 82.5% and testing accuracy of 83.33% that reached in (Jiang et al. 2020), we have raised these two accuracies by 16.24% and 14.20%, respectively. Figure 10 shows the classification

Table 2. Splitting data.

Data	Label 1	Label 2	Label 3	Label 4	Label 5
Training data	0.8×205	0.8×74	0.8×52	0.8×39	0.8×30
Testing data	0.2×205	0.2×74	0.2×52	0.2×39	0.2×30

Table 3. Validation accuracy for each model.

ML model	V_1	V_2	V_3	V_4	V_5	Mean (V)
DNN1	0.9836	1.0	1.0	0.9692	0.9538	0.9813
DNN2	0.9344	1.0	1.0	0.9846	1.0	0.9838
DNN3	0.9672	1.0	1.0	0.9846	0.9692	0.9842
SVM	0.9344	0.9687	0.9687	0.923	0.9384	0.9466
DT	0.9508	0.9531	1.0	0.9846	0.9692	0.9715
RF	1.0	0.9531	1.0	0.9692	0.9538	0.9752
LR	0.8852	0.9062	0.9375	0.8615	0.9076	0.8996

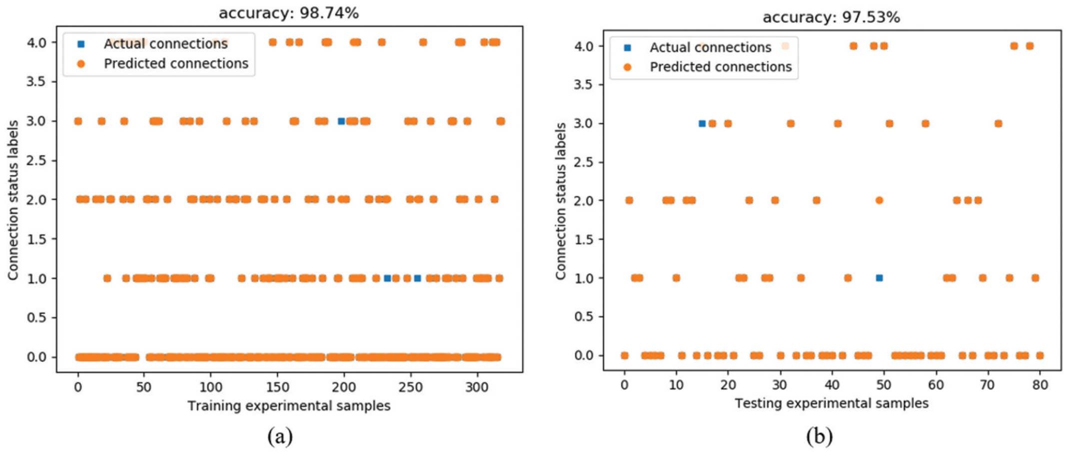

Figure 10. Classification performance, (a) on training dataset and (b) on testing dataset.

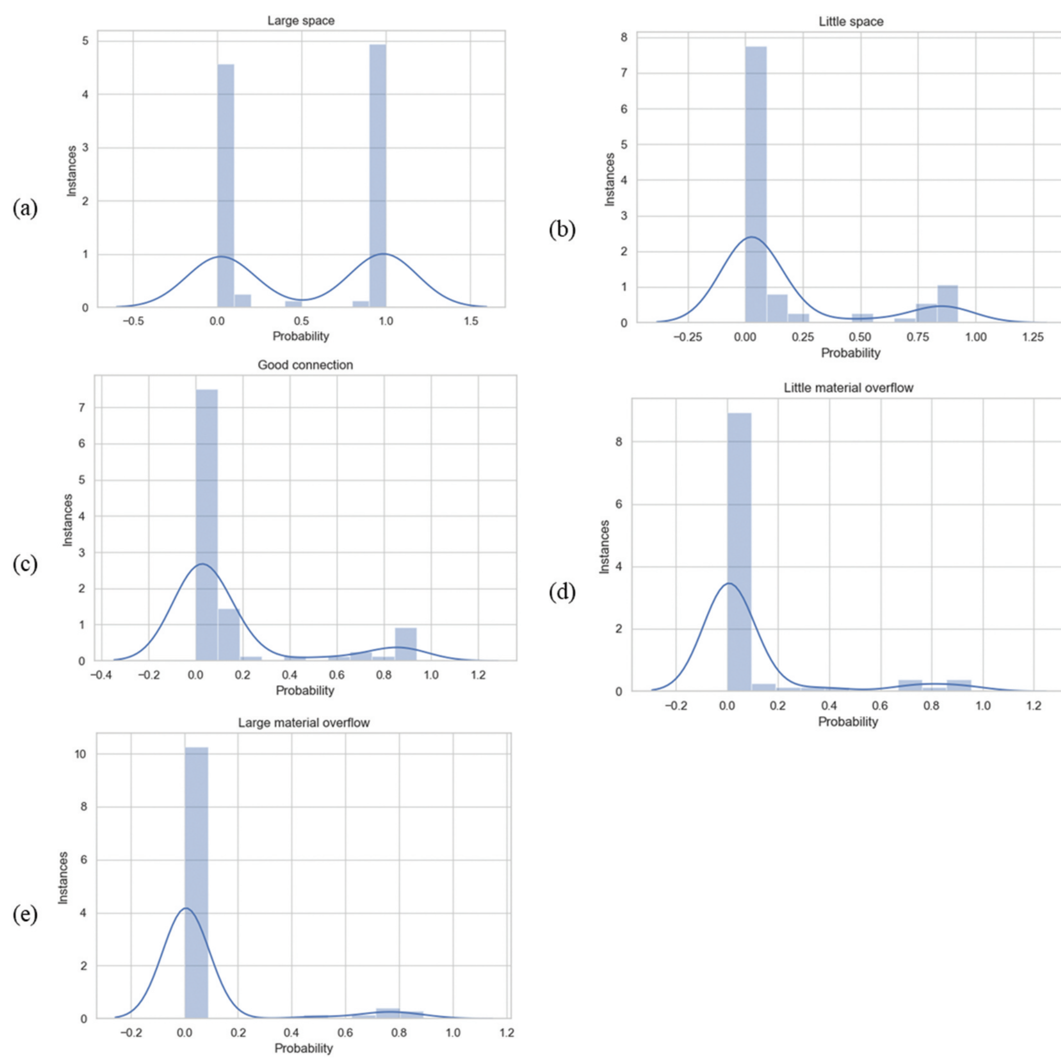

Figure 11. Probability distributions (a) large space (b) little space (c) good connection (d) little material overflow (e) large material overflow.

performance of DNN3 on the training and testing data. Blue color squares represent actual connection statuses, and orange color circles represent the predicted connection statuses. It is seen that squares and circles are overlapped in many of instances. The overlapping tells us that actual class label is equal to the predicted one. This assures that DNN3 identifies the connection status very well.

The proposed open-loop classification model achieves our first objective, i.e. revealing the relationship between processing parameters and the printed part properties. From the classification results, the connection status of printed parts for the corresponding processing parameters is known. Consequently, we are clear which processing parameters result in a good connection between the printed lines in an offline manner.

Moreover, a five-level connection status probability distribution is generated by making testing data as input to DNN3. The 10-bin histogram-based graphical representation of connection statuses, including 'Large space', 'Little space', 'Good connection', 'Little material overflow', and 'Large material overflow' are shown in Figure 11(a–e) respectively. In Figure 11, the connection status probabilities are presented in increasing order as Large material overflow, Little material overflow, Good connection, Little space, and Large space. We have observed that a 'Large space' occurred in most of instances for our testing data. This shows that the proposed open-loop classification approach tells us only the status of the printed parts without any processing parameters adjustment. Therefore, incorporating a process monitoring system is required to optimize the effect of processing parameters on the quality of printed parts. From the knowledge of open-loop classification results, we can realize our second objective to design a closed-loop control system to generate optimal processing parameters. The proposed closed-loop system is analyzed next.

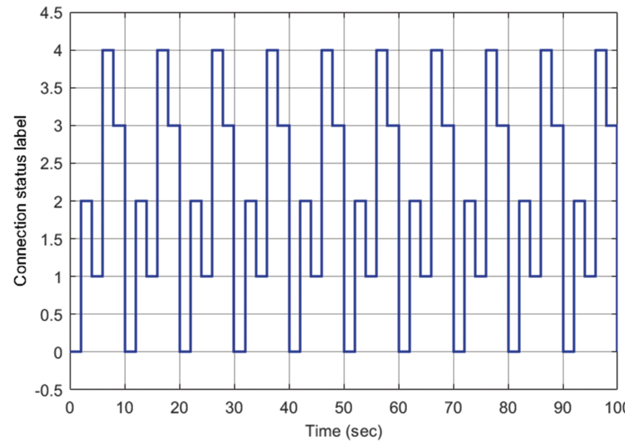

Figure 12. Connection status setting.

5.2. Closed-loop analysis

In this section, the simulation results and discussions of the proposed closed-loop control system are presented. A feedback control system that comprises open-loop ML model, fuzzy inference system,

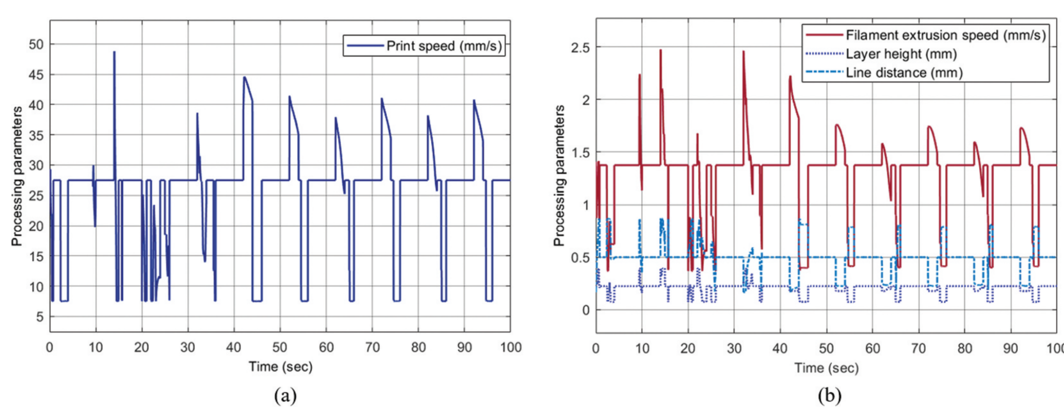

Figure 13. Optimized processing parameters, (a) print speed and (b) the other three parameters.

extruder system, and comparator is analyzed. Inputs to the comparator are reference and actual connection status information, and the comparator returns an error as an output. The fuzzy system takes 'Error' and 'Change in error' as input and generates the optimized processing parameters that drive the extruder system. The fuzzy inference rules are constructed from a priori-knowledge of the open-loop ML model.

The feedback system simulation is run for 100 seconds. At the very beginning of the printing process, a 3D printer is assumed to run under initial processing parameters that correspond to an initial printed line connection. However, the initial one may not be the desired one. Therefore, we assign different types of connection statuses as a reference, and the objective is to track the best connection status after some printing time. Figure 12 shows the five-level connection statuses that are given to the control algorithm which could be used as a reference. Following that, the corresponding processing parameters that may be different from the initial processing parameters are generated from the simulation of the feedback control system. Figure 13 shows the output of the designed control algorithm, which are named as the optimized processing parameters, including layer height, print speed, line distance, and filament extrusion speed in the function of time. The new optimized processing parameters thus drive the printing system to result in a good connection between the printed lines. We observe that the quality of connections between printed lines gets improved by introducing the control loop in the entire 3D printing process. Figure 14 shows the actual connection status that basically characterizes the quality of a 3D printing system. It is observed that after 25 seconds the connection status is approaching to class 2, which is good connection status. Despite the fact that the connection status profile is centered on 1.5, the majority of the profile touches class 2 and the remainder touches class 1. This is due to the fact that the 3D printing process is dynamic and difficult to be steady in terms of printed part properties. The optimized processing parameters generate better printed part properties at a time and the printing process may not sustain longer due to a variety of reasons such as environmental disturbances, equipment problems, and so on. That is why the profile touches class 2 once and class 1 the other time. This tells us about the quality assuring capability of the proposed closed-loop system. Generally speaking, the fuzzy system monitors the overall printing process by using the fuzzy rules. Moreover, the proposed feedback system plays a vital role in generating optimized control actions and at the same time it ensures the printing quality.

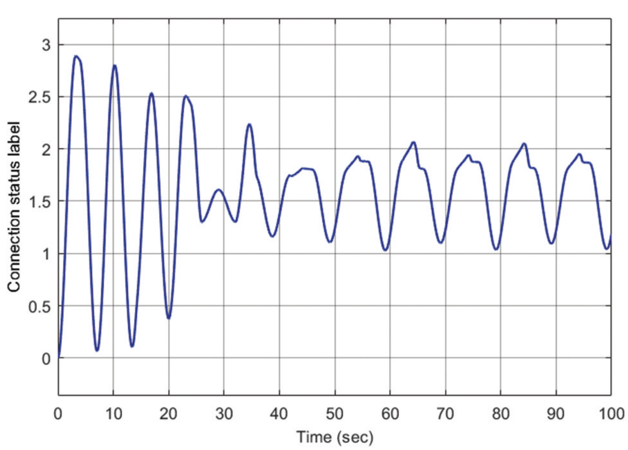

Figure 14. Actual connection status.

It can be said that performances of the proposed open-loop and closed-loop approaches mainly rely on an accurate ML algorithm. The nicely tuned ML algorithm results in a good classification performance. Furthermore, it is shown that the integration of ML with feedback control plays a vital role in achieving good connection between the printed lines in 3D printing. Although the proposed closed-loop algorithm cannot find an optimal processing parameter in the early stage of the printing process, it tolerates some recommended time and tracks the best connection status.

Last, since AM is a fast growing technology in the domain of digital manufacturing, proposing a novel control framework is a vital component for assuring the quality of products. Far from the existing open-loop control techniques applied to most of the existing AM processes, our control framework integrates both open-loop and closed-loop techniques and improves the performance of the 3D printing process by generating the optimized processing parameters. The proposed control system approach gives a promising result for growing AM technologies further. Therefore, it is recommended for practitioners to apply this practical concept for building advanced 3D printing equipment.

6. Conclusion

Given the issue of quality and mechanical strength of printed parts in AM industry, this paper presents a mechanism to monitor processing parameters, including layer height, print speed, line distance, and filament extrusion speed via ML algorithms. Two types of control frameworks are proposed to monitor processing parameters. 1) Open-loop approach: five ML classification algorithms that generate the relationship between processing parameters and printed part properties are presented. Among which, DNN3 performs better than others and is thus chosen as the final classification model in this work. Consequently, this ML model can identify the best processing parameters combinations that result better printed part quality in an offline manner. Furthermore, this ML model can be applied to design a closed-loop control system. 2) Closed-loop approach: a fuzzy logic-based feedback control system along with the mathematical model of a 3D printer is designed to generate four optimized processing parameters. In this regard, the fuzzy system monitors the overall printing process via fuzzy rules which characterizes the values of processing parameters. It can be said that a closed-loop ML algorithm has good contribution to the monitoring and optimization of processing parameters in 3D printing, thus significantly improving the quality of printed part properties. As a result, a self-adjusting 3D printing system can be formed in the entire printing process and this fact leads to grow AM one step further. Last, it is observed that this work uses only adjustable processing parameters to maintain the quality of printed parts. Therefore, as recommendation, the quality of a printed part can be further improved if additional processing parameters are considered. Moreover, the results can be improved and complemented by refining the control and optimization frameworks. The next step is to do real-time closed-loop 3D printing experiments.

Nomenclature

3D	Three Dimensional
AM	Additive Manufacturing
CAD	Computer Aided Design
DNN	Deep Neural Network
DT	Decision Tree
FLC	Fuzzy Logic Controller
LR	Logistic Regression
ML	Machine Learning
MVLR	Multi-Variate Linear Regression
NN	Neural Network
RF	Random Forest
SVM	Support Vector Machine
WAAM	Wire and Arc Additive Manufacturing

Disclosure statement

No potential conflict of interest was reported by the author(s).

Funding

This work was supported in part by the National Key Research and Development Program of China (No. 2018YFB1700403); National Natural Science Foundation of China under Grants U1909204, U1909218, U1811463, 61872365 & 61806198; CAS Key Technology Talent Program (Zhen Shen); The Guangdong Basic and Applied Basic Research Foundation under Grant 2021B1515140034; The Foshan Science and Technology Innovation Team Project under Grant 2018IT100142; The Scientific Instrument Developing Project of the Chinese Academy of Sciences under Grant No. YZQT014; CAS STS Dongguan Joint Project 20201600200072

ORCID

Tariku Sinshaw Tamir http://orcid.org/0000-0003-3700-928X
Gang Xiong http://orcid.org/0000-0002-4303-5559
Zhen Shen http://orcid.org/0000-0002-9634-4945
MengChu Zhou http://orcid.org/0000-0002-5408-8752
Jingchao Jiang http://orcid.org/0000-0002-0446-3454

References

Bikas, H., P. Stavropoulos, and G. Chryssolouris. 2016. “Additive Manufacturing Methods and Modelling Approaches: A Critical Review.” *International Journal of Advanced Manufacturing Technology* 83 (1–4): 389–405. doi:10.1007/s00170-015-7576-2.

Bin Ishak, Ismayuzri, David Fleming, and P. Larochelle. 2019. “Multiplane Fused Deposition Modeling: A Study of Tensile Strength.” *Mechanics Based Design of Structures and Machines* 47 (5): 583–598. doi:10.1080/15397734.2019.1596127.

Camacho, D. D., P. Clayton, W. J. O’Brien, C. Seepersad, M. Juenger, R. Ferron, and S. Salamone. 2018. “Applications of Additive Manufacturing in the Construction Industry–A

Forward-Looking Review." *Automation in Construction* 89: 110–119. doi:10.1016/j.autcon.2017.12.031.

Cao, Z., C. Lin, and M. Zhou. 2021. "A Knowledge-Based Cuckoo Search Algorithm to Schedule a Flexible Job Shop with Sequencing Flexibility." *IEEE Transactions on Automation Science and Engineering* 18 (1): 56–69.

Ding, D., Z. Pan, D. Cuiuri, and H. Li. 2015. "A Practical Path Planning Methodology for Wire and Arc Additive Manufacturing of Thin-Walled Structures." *Robotics and Computer-Integrated Manufacturing* 34: 8–19. doi:10.1016/j.rcim.2015.01.003.

Di, L., T. Srikanthan, R.S. Chandel, and I. Katsunori. 2001. "Neural-Network-Based Self- Organized Fuzzy Logic Control for Arc Welding." *Engineering Applications of Artificial Intelligence* 14 (2): 115–124. doi:10.1016/S0952-1976(00)00057-9.

Esmaeilian, B., S. Behdad, and B. Wang. 2016. "The Evolution and Future of Manufacturing: A Review." *Journal of Manufacturing Systems* 39: 79–100. doi:10.1016/j.jmsy.2016.03.001.

Fang, Q., G. Xiong, M. Zhou, T. S. Tamir, C.-B. Yan, H. Wu, Z. Shen, and F. Y. Wang, "Process Monitoring, Diagnosis and Control of Additive Manufacturing," IEEE Transactions on Automation Science and Engineering, to appear in 2023.

Feng, J., J. Fu, Z. Lin, C. Shang, and B. Li. 2018. "Direct Slicing of T-Spline Surfaces for Additive Manufacturing." *Rapid Prototyping Journal* 24 (4): 709–721. doi:10.1108/RPJ-12-2016-0210.

Francis, J., and L. Bian. 2019. "Deep Learning for Distortion Prediction in Laser-Based Additive Manufacturing Using Big Data." *Manufacturing Letters* 20: 10–14. doi:10.1016/j.mfglet.2019.02.001.

Geron, A. 2018. *Hands-On Machine Learning with Scikit-Learn and Tensor Flow*. Sebastopol, CA, United States: O'Reily Media Inc.

Ghahramani, M., Y. Qiao, M. Zhou, A. O. Hagan, and J. Sweeney. 2020. "AI-Based Modeling and Data-Driven Evaluation for Smart Manufacturing Processes." *IEEE/CAA Journal of Automatica Sinica* 7 (4): 1026–1037. doi:10.1109/JAS.2020.1003114.

Goh, G.D., S.L. Sing, and W.Y. Yeong. 2020. "A Review on Machine Learning in 3D Printing: Applications, Potential, and Challenges." *Artificial Intelligence Review* 54 (1): 1–32. doi:10.1007/s10462-020-09876-9.

Goodfellow, I., Y. Bengio, A. Courville, and Y. Bengio. 2016. *Deep Learning*. Vol. 1. Cambridge, Massachusetts (United States): MIT press Cambridge.

Heidarzadeh, A., Ö. Müge Testik, G. Güleryüz, and R. Vatankhah Barenji. 2020. "Development of a Fuzzy Logic Based Model to Elucidate the Effect of FSW Parameters on the Ultimate Tensile Strength and Elongation of Pure Copper Joints." *Journal of Manufacturing Processes* 53: 250–259. doi:10.1016/j.jmapro.2020.02.020.

Huang, B., and S. B. Singamneni. 2015. "Curved Layer Adaptive Slicing (CLAS) for Fused Deposition Modelling." *Rapid Prototyping Journal* 21 (4): 354–367. doi:10.1108/RPJ-06-2013-0059.

Ieracitano, C., A. Paviglianiti, M. Campolo, A. Hussain, E. Pasero, and F. Carlo Morabito. 2020. "A Novel Automatic Classification System Based on Hybrid Unsupervised and Supervised Machine Learning for Electrospun Nanofibers." *IEEE/CAA Journal of Automatica Sinica* 8 (1): 64–76. doi:10.1109/JAS.2020.1003387.

Isa, M. A., and I. Lazoglu. 2019. "Five-Axis Additive Manufacturing of Freeform Models Through Buildup of Transition Layers." *Journal of Manufacturing Systems* 50: 69–80. doi:10.1016/j.jmsy.2018.12.002.

Jiang, J. 2019. "Machine Learning for Additive Manufacturing". Accessed 20 August 2020. http://www.github.com/jjia547/ML-for-AM

Jiang, J., C. Yu, X. Xu, Y. Ma, and J. Liu. 2020. "Achieving Better Connections Between Deposited Lines in Additive Manufacturing via Machine Learning." *Mathematical Biosciences and Engineering* 17 (4): 3382. doi:10.3934/mbe.2020191.

Jin, Y., J. Du, Y. He, and G. Fu. 2017. "Modeling and Process Planning for Curved Layer Fused Deposition." *International Journal of Advanced Manufacturing Technology* 91 (1–4): 273–285. doi:10.1007/s00170-016-9743-5.

Khanzadeh, M., S. Chowdhury, M. Marufuzzaman, M. A. Tschopp, and L. Bian. 2018. "Porosity Prediction: Supervised-Learning of Thermal History for Direct Laser Deposition." *Journal of Manufacturing Systems* 47: 69–82. doi:10.1016/j.jmsy.2018.04.001.

Khargonekar, P. P., and M. A. Dahleh. 2018. "Advancing Systems and Control Research in the Era of ML and AI." *Annual Reviews in Control* 45: 1–4.

Li, Yongzhe, X. Li, G. Zhang, I. Horváth, and Q. Han. 2021. "Interlayer Closed-Loop Control of Forming Geometries for Wire and Arc Additive Manufacturing Based on Fuzzy-Logic Inference." *Journal of Manufacturing Processes* 63: 35–47.

Lim, S., R. A. Buswell, P. J. Valentine, D. Piker, S. A. Austin, and X. De Kestelier. 2016. "Modelling Curved-Layered Printing Paths for Fabricating Large- Scale Construction Components." *Additive Manufacturing* 12: 216–230.

Liu, H.-C., X. Luan, M. Zhou, and Y. Xiong. 2020. "A New Linguistic Petri Net for Complex Knowledge Representation and Reasoning." *IEEE Transactions on Knowledge and Data Engineering* 34 (3): 1011–1020. doi:10.1109/TKDE.2020.2997175.

Li, Zhixiong, Z. Zhang, J. Shi, and D. Wu. 2019. "Prediction of Surface Roughness in Extrusion-Based Additive Manufacturing with Machine Learning." *Robotics and Computer-Integrated Manufacturing* 57: 488–495.

Mei, J., Z. Lu, J. Hu, and Y. Fan. 2021. "Energy-Efficient Optimal Guaranteed Cost Intermittent-Switch Control of a Direct Expansion Air Conditioning System." *IEEE/CAA Journal of Automatica Sinica* 8 (11): 1852–1866.

Meng, L., B. McWilliams, W. Jarosinski, H. Yeong Park, Y. Gil Jung, J. Lee, and J. Zhang. 2020. "Machine Learning in Additive Manufacturing: A Review." *JOM* 72: 2363–2377. doi:10.1007/s11837-020-04155-y.

Moe, S., A. Marthine Rustad, and K. G. Hanssen. 2018. "Machine Learning in Control Systems: An Overview of the State of the Art." In *International Conference on Innovative Techniques and Applications of Artificial Intelligence*, 250–265. Springer International Publishing, Cham: Springer.

Ngo, T. D., A. Kashani, G. Imbalzano, K. T. Nguyen, and D. Hui. 2018. "Additive Manufacturing (3D Printing): A Review of Materials, Methods, Applications and Challenges." *Composites Part B: Engineering* 143: 172–196.

Popova, E., T. M. Rodgers, X. Gong, A. Cecen, J. D. Madison, and S. R. Kalidindi. 2017. "Process-Structure Linkages Using a Data Science Approach: Application to Simulated Additive Manufacturing Data." *Integrating Materials and Manufacturing Innovation* 6 (1): 54–68.

Prieto-Entenza, P. J., N. Ramon Cazarez-Castro, L. T. Aguilar, S. L. Cardenas- Maciel, and J. Antonio Lopez-Renteria. 2019. "A Lyapunov Analysis for Mamdani Type Fuzzy-Based Sliding Mode Control." *IEEE Transactions on Fuzzy Systems* 28 (8): 1887–1895.

Qi, X., G. Chen, Y. Li, X. Cheng, and C. Li. 2019. "Applying Neural-Network-Based Machine Learning to Additive Manufacturing: Current Applications, Challenges, and Future Perspectives." *Engineering* 5 (4): 721–729.

Shen, Z., X. Shang, Y. Li, Y. Bao, X. Zhang, X. Dong, L. Wan, G. Xiong, and F.-Y. Wang. 2019a. "PredNet and CompNet: Prediction and High-Precision Compensation of In-Plane Shape Deformation for Additive Manufacturing." In *2019 IEEE 15th International Conference on Automation Science and Engineering (CASE)*, Vancouver, BC, Canada, 462–467. IEEE.

Shen, Z., X. Shang, M. Zhao, X. Dong, G. Xiong, and F.-Y. Wang. 2019b. "A Learning-Based Framework for Error Compensation in 3D Printing." *IEEE Transactions on Cybernetics* 49 (11): 4042–4050.

Sugiyama, K., R. Matsuzaki, M. Ueda, A. Todoroki, and Y. Hirano. 2018. "3D Printing of Composite Sandwich Structures Using Continuous Carbon Fiber and Fiber Tension." *Composites Part A, Applied Science and Manufacturing* 113: 114–121.

Tamir, T. S., G. Xiong, X. Dong, Q. Fang, S. Liu, E. Lodhi, Z. Shen, and F.-Y. Wang. 2022a. "Design and Optimization of a Control Framework for Robot Assisted Additive Manufacturing Based on the Stewart Platform." *International Journal of Control, Automation, and Systems* 20 (3): 968–982.

Tamir, T. S., G. Xiong, Q. Fang, X. Dong, Z. Shen, and F.-Y. Wang. 2022b. "A Feedback-Based Print Quality Improving Strategy for FDM 3D Printing: An Optimal Design Approach." *International Journal of Advanced Manufacturing Technology* 120 (3): 2777–2791.

Tamir, T. S., G. Xiong, Z. Li, H. Tao, Z. Shen, B. Hu, and H. Mulugeta Menkir. 2020a. "Traffic Congestion Prediction Using Decision Tree, Logistic Regression and Neural Networks." *Ifac-PapersOnline* 53 (5): 512–517.

Tamir, T. S., G. Xiong, H. Mulugeta Menkir, X. Shang, Z. Shen, X. Dong, and X. Gong. 2020b. "Developing SCADA Systems to Monitor and Control Liquid and Detergent Factories." In *2020 IEEE 16th International Conference on Automation Science and Engineering (CASE)*, Hong Kong, China, 691–696. IEEE.

Tamir, T. S., G. Xiong, Z. Shen, X. Gong, S. Liu, E. Lodhi, L. Wan, and X. Dong. 2020c. "Comparative Study of Four Speed Controllers of Brushless DC Motors for Industrial Applications." *Ifac-PapersOnline* 53 (5): 59–64.

Uhlmann, E., A. Bergmann, R. Bolz, and W. Gridin. 2018. "Application of Additive Manufactured Tungsten Carbide Tool Electrodes in EDM." *Procedia CIRP* 68: 86–90.

Wang, F., S. Fathizadan, F. Ju, K. Rowe, and N. Hofmann. 2021. "Print Surface Thermal Modeling and Layer Time Control for Large-Scale Additive Manufacturing." *IEEE Transactions on Automation Science and Engineering* 18 (1): 244–254.

Wang, T., T.-H. Kwok, C. Zhou, and S. Vader. 2018b. "In-Situ Droplet Inspection and Closed-Loop Control System Using Machine Learning for Liquid Metal Jet Printing." *Journal of Manufacturing Systems* 47: 83–92.

Wang, J., Y. Ma, L. Zhang, R. X. Gao, and D. Wu. 2018a. "Deep Learning for Smart Manufacturing: Methods and Applications." *Journal of Manufacturing Systems* 48: 144–156.

Wang, C., W. Pedrycz Z. Li, and M. Zhou. 2021. "Residual-driven Fuzzy C-Means Clustering for Image Segmentation." *IEEE/CAA Journal of Automatica Sinica* 8 (4): 876–889.

Xia, L., S. Lin, and G. Ma. 2020. "Stress-Based Tool-Path Planning Methodology for Fused Filament Fabrication." *Additive Manufacturing* 32: 101020.

Xie, F., L. Chen, Z. Li, and K. Tang. 2020. "Path Smoothing and Feed Rate Planning for Robotic Curved Layer Additive Manufacturing." *Robotics and Computer-Integrated Manufacturing* 65: 101967.

Xiong, G., T. S. Tamir, Z. Shen, X. Shang, H. Wu, and F. Y. Wang. 2022. "A Survey on Social Manufacturing: A Paradigm Shift for Smart Prosumers," IEEE Transactions on Computational Social Systems. doi:10.1109/TCSS.2022.3180201.

Yao, S., Q. Kang, M. Zhou, M. J. Rawa, and A. Abusorrah. 2022. "A Survey of Transfer Learning for Machinery Diagnostics and Prognostics." *Artificial Intelligence Review*. doi:10.1007/s10462-022-10230-4.

Zadeh, L. A. 1965. "Fuzzy Sets." *Information and Control* 8 (3): 338–353.

Zhang, H., Y. Yang, K. Hu, B. Liu, M. Liu, and Z. Huang. 2020. "Stereolithography-Based Additive Manufacturing of Lightweight and High-Strength Cf/SiC Ceramics." *Additive Manufacturing* 34: 101199.

Zhao, G., G. Ma, J. Feng, and W. Xiao. 2018. "Nonplanar Slicing and Path Generation Methods for Robotic Additive Manufacturing." *International Journal of Advanced Manufacturing Technology* 96 (9–12): 3149–3159.

Zhao, M., G. Xiong, X. Shang, C. Liu, Z. Shen, and H. Wu. 2019. "Nonlinear Deformation Prediction and Compensation for 3D Printing Based on CAE Neural Networks." In *2019 IEEE 15th International Conference on Automation Science and Engineering (CASE)*, Vancouver, BC, Canada, 667–672. IEEE.